Statistical bias in periodograms derived from solar wind time series

J. J. Podesta[1]

Received 16 May 2005; revised 8 March 2006; accepted 13 March 2006; published 19 July 2006.

[1] The bias in periodogram spectral estimators is computed as a function of the sample size N by assuming a model power spectrum that decays like $f^{-\alpha}$ at high frequencies. For $\alpha = 2$, it is shown that when the aliasing of the measured power spectrum is properly taken into account the bias in the "raw" periodogram is nearly independent of frequency for large N. For the range of values $1.7 \lesssim \alpha < 2$, an upper bound on the bias is provided by the case $\alpha = 2$. Theoretical calculations of the maximum absolute bias as a function of N are used to determine when the periodogram is approximately unbiased and when the bias is significant enough to require the use of a modified periodogram which incorporates data tapering, also called data windowing. For solar wind velocity data acquired by the ACE spacecraft and a chosen low frequency cutoff of 10^{-7} Hz, the bias in periodogram spectral estimators is found to be less than 4% for sample sizes N greater than $2^{16} = 65536$. This corresponds to a 49 day record of 64 s data.

Citation: Podesta, J. J. (2006), Statistical bias in periodograms derived from solar wind time series, *J. Geophys. Res.*, *111*, A07103, doi:10.1029/2005JA011233.

1. Introduction

[2] Calculations of power spectra based on a single periodogram without a data taper or data window may be significantly biased. It has long been known that for stationary stochastic processes with power spectra characterized by a large dynamic range, the "raw" periodogram may exhibit large biases, even for very large sample sizes N [*Percival and Walden*, 1993; *Thomson*, 1977]. It is also well known that such biases may be reduced by employing a modified periodogram that includes a data taper or data window or by using more advanced nonparametric techniques such as the multitaper method [*Thomson*, 1982; *Percival and Walden*, 1993].

[3] The important question is: for a given time series with a particular spectrum, how large must N be chosen so that the bias errors in the periodogram are negligible? Or, in other words, for what values of N is tapering unnecessary? These considerations are important for improving the precision of spectral estimates and for the accurate estimation of power law indices such as those observed in the solar wind. The latter issue is of fundamental importance in solar wind physics and in the theory of turbulence in collisionless magnetized plasmas [*Goldstein and Roberts*, 1999].

[4] The bias error of a spectral estimator $\hat{S}(f)$ is the amount by which the first moment of the estimator differs from the true power spectral density $S(f)$. If the two are equal so that

$$E\{\hat{S}(f)\} = S(f), \tag{1}$$

where E denotes the mathematical expectation, then $\hat{S}(f)$ is called an unbiased estimator of the power spectrum $S(f)$. The difference $E\{\hat{S}(f)\} - S(f)$ is called the bias of the estimator $\hat{S}(f)$.

[5] The bias error is a local property, that is, it is a function of the frequency f. If the spectrum is continuous and slowly varying in the neighborhood of a point f_0, then a constant offset between the expectation $E\{\hat{S}(f)\}$ and the power spectrum $S(f)$ gives rise to a constant bias in the neighborhood of f_0. In general, the first moment of the periodogram spectral estimator may be expressed in the form

$$E\{\hat{S}_N(f)\} = \int_{-f_{NQ}}^{f_{NQ}} S(f') F_N(f - f')\, df', \tag{2}$$

where $f_{NQ} = 1/2\Delta t$ is the Nyquist frequency and

$$F_N(f) = \frac{\Delta t \sin^2(N\pi f \Delta t)}{N \sin^2(\pi f \Delta t)} \tag{3}$$

is the Fejér kernel [see *Priestley*, 1981, equation 6.2.11 or *Percival and Walden*, 1993, equation 198c]. Equation (2) shows that the first moment is a "smoothed" version of $S(f')$ obtained by first multiplying by the approximate delta function $F_N(f - f')$ and then integrating with respect to f'. As a consequence, if $S(f)$ contains a narrow peak at the frequency f_0, then the first moment (2) contains a smoothed peak having a wider line width and reduced amplitude. In this example, the bias in the neighborhood of f_0 is frequency dependent.

[6] The purpose of this study is to explicitly compute the bias error for a model power spectrum and to show that for high pass filtered solar wind velocity data with a low-

[1]Laboratory for Solar and Space Physics, NASA Goddard Space Flight Center, Greenbelt, Maryland, USA.

0148-0227/06/2005JA011233

frequency cutoff of 10^{-7} Hz and a sampling period of 64 s, the bias in the raw periodogram is negligible for values of N on the order of 3×10^4. More specifically, the bias is less than 8% for all frequencies of interest if $N > 2^{15} = 32768$ and the bias is less than 4% for all frequencies of interest if $N > 2^{16} = 65536$. For such large values of N, data windows are probably unnecessary. However, for smaller values of N, the bias in the periodogram should probably be reduced by using data tapering or some other technique.

[7] While the results presented here pertain to solar wind velocity data obtained at 1 AU in the ecliptic plane by the SWEPAM instrument on board NASA's Advanced Composition Explorer (ACE) [*McComas et al.*, 1998] the same analysis method may be applied to any time series possessing similar spectral characteristics in the observed frequency range.

2. Method of Analysis

[8] The periodogram is an asymptotically unbiased spectral estimator in the limit as the sample size N approaches infinity. In practice, however, it is necessary to know how large N must be chosen in order for the bias to be negligible. One way to estimate N is to assume a specific functional form for the power spectrum $S(f)$ and then directly compute the bias

$$E\{\hat{S}_N(f)\} - S(f) \tag{4}$$

as a function of N and f. This is the approach adopted here. In equation (4), the expectation operator E denotes the ensemble average (mathematical expectation) and

$$\hat{S}_N(f) = \frac{\Delta t}{N}\left|\sum_{n=0}^{N-1} X_n\, e^{-i2\pi n f \Delta t}\right|^2 \tag{5}$$

is the periodogram for the sample $X_0, X_1, \ldots, X_{N-1}$ of size N.

[9] For solar wind data that has been high pass filtered with a filter cutoff frequency of 10^{-7} Hz in order to remove any DC component or slowly varying trends while passing the fundamental solar rotation frequency 4.3×10^{-7} Hz, the spectrum can be crudely approximated by the function

$$S(f) = \frac{S_0}{1 + |f/f_0|^{\alpha}}, \tag{6}$$

where S_0 is constant, $f_0 = 10^{-6}$ Hz, and $\alpha \approx 1.7$. Previous experience with solar wind spectra at 1 AU suggests that this is a reasonable hypothesis for frequencies in the turbulent inertial range where typically $\alpha \simeq 1.7$ [*Bavassano et al.*, 1982; *Goldstein et al.*, 1995; *Goldstein and Roberts*, 1999; *Leamon et al.*, 1998; *Marsch*, 1991; *Matthaeus and Goldstein*, 1982; *Tu and Marsch*, 1995]. For mathematical simplicity, it is convenient to choose the value $\alpha = 2$ in equation (6) since the results obtained are not expected to be sensitive to the precise value of α. This is checked later in section 3.

[10] As a consequence of high pass filtering, the spectrum actually vanishes at $f = 0$. This is neglected in the model (6) because it does not significantly effect the bias for frequencies in the passband. In fact, the approximation of a flat spectrum near $f = 0$ in equation (6) can only increase the bias for frequencies in the passband.

[11] Assuming that the observed stochastic process possesses the power spectrum (6), then, after sampling, the sampled power spectrum takes the form

$$S_a(f) = \sum_{n=-\infty}^{\infty} S(f - nf_s), \tag{7}$$

where $f_s = 1/\Delta t$ is the sampling frequency and $S(f)$ is given by equation (6). Equation (7) shows that the sampled power spectrum contains aliasing. The subscript "a" stands for "aliased." The aliased power spectrum (7) is the power spectrum which one is attempting to estimate from the data. In the case $\alpha = 2$, the infinite series (7) can be computed in closed form using the theory of residues [*Levinson and Redheffer*, 1970] with the result

$$S_a(f) = \frac{\pi S_0 f_0 \Delta t}{\tanh(\pi f_0 \Delta t)\cos^2(\pi f \Delta t) + \mathrm{ctnh}(\pi f_0 \Delta t)\sin^2(\pi f \Delta t)}, \tag{8}$$

where $|f| \leq 1/(2\Delta t)$. It should be noted that this is equivalent to the spectrum of a first order autoregressive process, namely,

$$S_a(f) = \frac{\sigma_1^2 \Delta t}{|1 - \phi e^{-i2\pi f \Delta t}|^2}, \tag{9}$$

where $\sigma_1^2 = \pi f_0 S_0 (1 - \phi^2)$ and $\phi = e^{-2\pi f_0 \Delta t}$ [*Percival and Walden*, 1993, equation (392b)]. The latter form is derived from the discrete Fourier transform of the autocovariance sequence (11).

[12] It is important to note that the aliased power spectrum $S_a(f)$ is the correct spectrum to use when computing the bias (4). This is the power spectrum of the sampled signal, the signal actually measured. The two power spectra $S(f)$ and $S_a(f)$ are plotted in Figure 1 together with an unsmoothed periodogram obtained using ACE solar wind data at 1 AU. The periodogram was computed using a rectangular data window (no tapering) and a sample size of $N = 2^{18} = 262144$. ACE level II data for the period 1998 through 2004 were obtained from the ACE Science Center and preprocessed using linear interpolation to fill any missing data values followed by high pass filtering with a linear FIR filter having a cutoff frequency of 10^{-7} Hz. Those portions of the processed data containing filter transients were then deleted. The data used to compute the periodogram in Figure 1 spans approximately the first 6 months of 1999.

[13] Having determined an appropriate functional form for the power spectrum, the next task is to compute the expected value of the periodogram in equation (4). The expected value of the periodogram may be written

$$E\{\hat{S}_N(f)\} = \Delta t \sum_{n=-N}^{N-1}\left(1 - \frac{|n|}{N}\right) s_n\, e^{-i2\pi n f \Delta t}, \tag{10}$$

where s_n is the true autocovariance function of the (filtered) process [*Percival and Walden*, 1993, equation (198a)]. That

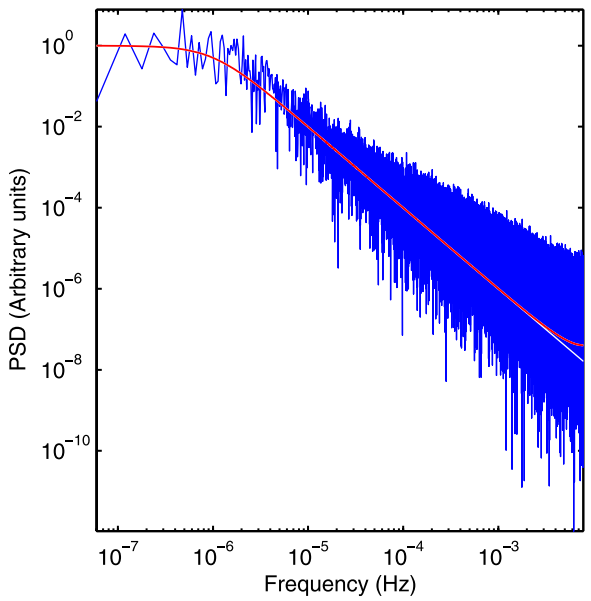

Figure 1. Periodogram of the radial solar wind velocity (blue) with $N = 2^{18} = 262144$, model power spectrum $S(f)$ (white), and aliased power spectrum $S_a(f)$ (red). The latter two functions are computed from equations (8) and (6) using $f_0 = 10^{-6}$ Hz and $\Delta t = 64$ s.

is, s_n is the inverse Fourier transform of equation (6) evaluated at the times $t = n\Delta t$. The inverse Fourier transform of $S(f)$ in equation (6) yields

$$s_n = \pi f_0 S_0 \, e^{-2\pi |n| f_0 \Delta t}, \tag{11}$$

where $-\infty < n < \infty$. For any value of N, the sum (10) is easily evaluated using standard fast Fourier transform (FFT) algorithms.

3. Results of the Calculations

[14] The relative (absolute) bias error, or normalized bias error, is conveniently represented in the form

$$\text{Bias Error} = \left| \frac{E\{\hat{S}_N(f)\} - S_a(f)}{S_a(f)} \right|, \tag{12}$$

where $E\{\hat{S}_N(f)\}$ is given by equation (10) and $S_a(f)$ is given by equation (8). Results for the computed bias error as a function of frequency are shown for three different values of N in Figure 2. The calculations extend all the way up to the Nyquist frequency $1/(2\Delta t) = 7.8 \times 10^{-3}$ Hz. The results indicate that, in general, the bias decreases as N increases. An important conclusion is that for fixed N, the relative bias is nearly a constant function of frequency except for a change in algebraic sign near $f_0 = 10^{-6}$ Hz.

[15] To show how the results in Figure 2 depend on the power law exponent α in equation (6), the bias error has been computed for the cases $\alpha = 1.9$, 1.8, and 1.7 by the methods described in Appendix A. Results for the sample size $N = 2^{16}$ are shown in Figure 3. At low frequencies the bias error is independent of α. Note that while the bias error is essentially independent of frequency in the case $\alpha = 2$, the

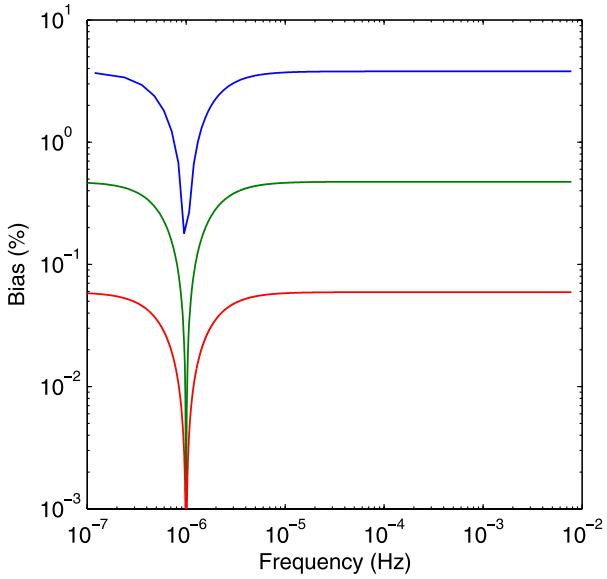

Figure 2. Bias error versus frequency for (top to bottom) $N = 2^{16} = 65536$, $N = 2^{19} = 524288$, and $N = 2^{22} = 4194304$.

bias error is a decreasing function of frequency for $\alpha < 2$ (neglecting the change in algebraic sign near $f_0 = 10^{-6}$ Hz). The important conclusion to be drawn from Figure 3 is that the case $\alpha = 2$ provides an upper bound for the bias error when $\alpha < 2$. It should be mentioned that the dip in the curve for $\alpha = 1.7$ that occurs near the Nyquist frequency in Figure 3 is probably not a real effect but the result of a loss of accuracy in the numerical calculations.

[16] The maximum bias error for the case $\alpha = 2$ is plotted as a function of N in Figure 4. Depending on how much bias one considers to be acceptable, Figure 4 can be used to determine the minimum sample size N needed to attain a

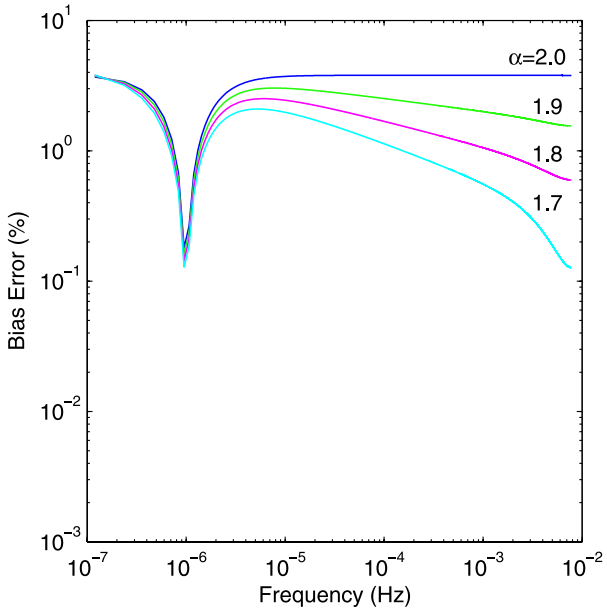

Figure 3. Bias error as a function of frequency for different power law exponents α in the power spectrum (6). The sample size is $N = 2^{16}$.

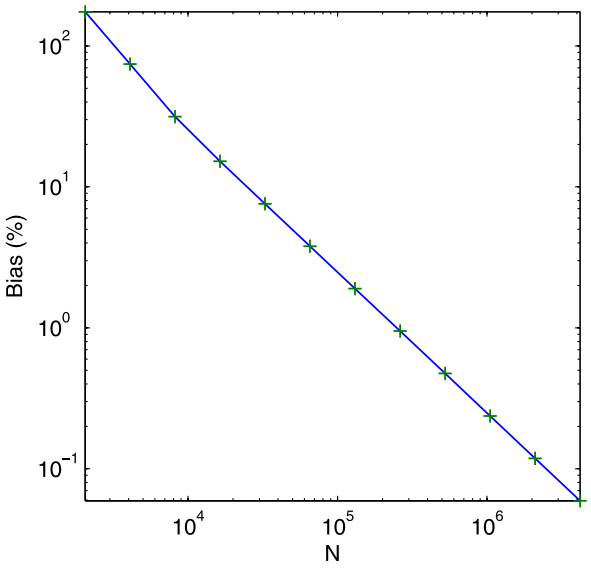

Figure 4. Maximum bias error in the raw periodogram as a function of the sample size N.

given level of bias for an unwindowed periodogram. For example, if $N \geq 2^{15} = 32768$, then the bias is less than 8%. This bias level is tolerable in many applications. A data record of size $N = 2^{15}$ corresponds to 24.27 days of ACE velocity data.

[17] For the practitioner of spectral estimation, the analysis presented in this paper is not the only way to evaluate the bias of a periodogram. A practical way to determine whether or not a periodogram may be biased is to compare spectral estimates obtained using different data tapers, or data windows, to spectral estimates obtained without using a data taper. If visual examination of the resulting spectra reveal no noticeable differences, then this suggests that the bias in the raw periodogram is probably negligible.

4. Discussion and Conclusions

[18] In summary, the bias error of the periodogram spectral estimator has been calculated as a function of the sample size N for a stationary, continuous time stochastic process with power spectrum (6) which is sampled at the rate Δt. Using parameters typical for ACE solar wind data ($\alpha \simeq 1.7$, $f_0 = 10^{-6}$ Hz, and $\Delta t = 64$ s), it was found that the bias errors become negligible for values of N on the order of 3×10^4. For values of N larger than this, the periodogram yields an approximately unbiased spectral estimate. For smaller values of N, the bias becomes significant and must be reduced by tapering or by other methods. It is important to note that throughout this study nothing has been said about the variance of the periodogram. The variance of the periodogram and variance reduction methods are not addressed in this paper.

[19] The analysis presented here shows that the effects of aliasing on the spectrum must be taken into account in order to correctly compute the bias. Without the effects of aliasing, that is, if $S(f)$ is used instead of $S_a(f)$ in equation (12), then the magnitude of the computed bias would be approximately 100% for frequencies near the Nyquist frequency (for the model spectrum studied here). Moreover, this result is practically independent of N. Therefore it is essential that the bias be measured relative to the aliased spectrum.

[20] It should be emphasized that the results shown in Figure 2 and 4 only apply to the special case of the power spectrum (6) with parameters $f_0 = 10^{-6}$ Hz and $\alpha = 2$, and for the sampling rate $\Delta t = 64$ s. For different values of the parameters f_0 and Δt the bias can be computed using the method described here, but the results would differ from those shown in Figure 2 and 4.

[21] In the case $\alpha \neq 2$, the approach used here is still applicable but requires more work as described in Appendix A. When $\alpha \neq 2$, equation (8) no longer applies and it is necessary to evaluate the sum (7) numerically. This can be done provided $\alpha \geq 1.7$ but is difficult for $\alpha < 1.7$. Computations for $1.7 \leq \alpha < 2$ indicate that the bias decreases as α decreases, so it is reasonable to conjecture that the case $\alpha = 2$ provides an upper bound on the bias for $1 < \alpha < 2$. For the computations, to evaluate the autocovariance function s_n of the process one must compute the inverse Fourier transform of equation (6). This can be done numerically using the FFT.

[22] Finally, it should be kept in mind that the smooth approximation of the spectrum given by equation (6) neglects any localized features which may be present in actual solar wind data such as spectral peaks at the solar rotation frequency 4.3×10^{-7} Hz and its harmonics. When such features are present in the data the bias errors will be different than the results obtained here, especially in the neighborhood of the spectral peaks. The effects of localized spectral features on the bias errors are not taken into account in this study.

Appendix A: Numerical Methods

[23] This appendix describes the numerical calculation of the bias error in the case when $\alpha \neq 2$, or, more specifically, when $1.7 \leq \alpha < 2$. The calculation is divided into two parts: the calculation of the aliased spectrum (7) and the calculation of the expected value of the periodogram, that is, equation (10). Because the bias (12) is the difference of two quantities that are approximately equal for large N, both terms must be computed with equal accuracy ε. Moreover, this accuracy must be much less than the bias error which is to be computed.

A1. Aliased Spectrum

[24] The aliased spectrum is given by

$$S_a(f) = \sum_{n=-\infty}^{\infty} \frac{S_0}{1 + (|f - nf_s|/f_0)^{\alpha}}, \tag{A1}$$

where $f_s = 1/\Delta t$ is the sampling frequency, $f_0 = 1 \times 10^{-6}$ Hz, and $|f| \leq f_{NQ} = f_s/2$. The terms of the series behave asymptotically like $1/|n|^{\alpha}$ as $n \to \infty$. Therefore like the series $\sum_{n=1}^{\infty} 1/n^{\alpha}$, the series (8) may be computed by truncation after N terms (provided α is not too close to 1). From the estimate

$$\sum_{n=N+1}^{\infty} \frac{1}{n^{\alpha}} \leq \int_{N+1}^{\infty} \frac{1}{(x - 1/2)^{\alpha}} dx = \int_{N+1/2}^{\infty} \frac{1}{x^{\alpha}} dx \leq \frac{1}{(\alpha - 1)N^{\alpha - 1}}, \tag{A2}$$

the truncation error for the series (8) is

$$\varepsilon_N \approx 2\left(\frac{f_0}{f_s}\right)^{\alpha} \sum_{n=N+1}^{\infty} \frac{1}{n^{\alpha}} \le 2\left(\frac{f_0}{f_s}\right)^{\alpha} \frac{1}{(\alpha-1)N^{\alpha-1}}. \quad \text{(A3)}$$

This truncation error is used below. Note that for the series $\sum_{n=1}^{\infty} 1/n^{\alpha}$, the relative error satisfies

$$\varepsilon = \frac{\sum_{n=N+1}^{\infty} 1/n^{\alpha}}{\sum_{n=1}^{\infty} 1/n^{\alpha}} \le \frac{\int_{N+1}^{\infty} (x-1/2)^{-\alpha}\, dx}{\int_{1}^{\infty} (x+1/2)^{-\alpha}\, dx} \le \left(\frac{3}{2N}\right)^{\alpha-1}. \quad \text{(A4)}$$

To evaluate the series (8) to within an error ε, proceed as follows. Let the relative error $\varepsilon > 0$ be given.

[25] 1. Set $N = (3/2)\varepsilon^{-1/(\alpha-1)}$ in accordance with equation (A4).

[26] 2. Evaluate the sum (7) by summing in reverse order, that is, from $|n| = N$ to $|n| = 0$.

[27] 3. Check that (ε_N/sum) $\le \varepsilon$, where ε_N is given by equation (A3).

[28] One should be careful not to allow N to become too large. This can happen when the desired error ε is too small. Even though the accumulation of roundoff errors is not a concern, it is a good idea in practice to limit N to 10^5 or 10^6. For the calculations that were performed to obtain Figure 3, $\varepsilon = 10^{-4}$.

A2. Expected Value of the Periodogram

[29] For $1.7 \le \alpha < 2$, the expected value of the periodogram $E\{\hat{S}_N(f)\}$ given by equation (10) is computed in two stages. First, the autocovariance function $s(\tau)$ is computed by evaluating the inverse Fourier transform of the power spectrum $S(f)$ in equation (6). This is accomplished by means of an FFT of length $2M$ as discussed below. In the second stage of the calculation, equation (10) is evaluated using an FFT of length $2N$ to compute the DFT of the sequence $(1 - |n|/N)s_n$, where $|n| \le N$. More details of the numerical methods are as follows.

[30] By symmetry, the autocovariance function may be written

$$s(\tau) = \int_{-f_c}^{f_c} S(f) \exp(i2\pi f\tau)\, df + 2\int_{f_c}^{\infty} S(f)\cos(2\pi f\tau)\, df, \quad \text{(A5)}$$

where f_c is a cutoff frequency introduced for the purpose of numerical calculation and the power spectrum $S(f)$ is defined by equation (6). If the cutoff frequency is made sufficiently large, then the error, given by the second term on the right-hand side of equation (A5), may be made as small as desired. The first integral in equation (A5) is then approximated by a Riemann sum to obtain

$$s(\tau) \approx \sum_{k=-M}^{M-1} S(f_k) \exp(-i2\pi f_k\tau)\Delta f, \quad \text{(A6)}$$

where $f_k = k\Delta f$ and $\Delta f = f_c/M$. The approximation of the first integral by a Riemann sum can be made as accurate as desired by increasing M. If the sum is evaluated at the times $\tau = n/2f_c$, then the previous equation becomes

$$s(\tau = n/2f_c) \approx \frac{f_c}{M} \sum_{k=-M}^{M-1} S(f_k) \exp(-i2\pi kn/2M). \quad \text{(A7)}$$

This is now in the standard form of the discrete Fourier transform (DFT) and is readily evaluated by means of the fast Fourier transform (FFT). The accuracy of the approximation (A7) is determined by the choice of f_c and M.

[31] To evaluate equation (10), the autocovariance function $s_n = s(n\Delta t)$ must be known at the times $\tau = n\Delta t$. From equation (A7), this implies that f_c must be a multiple of the Nyquist frequency $f_{NQ} = 1/2\Delta t$, that is, $f_c = mf_{NQ}$ where m is a positive integer. Furthermore, the entire time interval $(-N\Delta t, N\Delta t)$ covered by equation (10) must be contained in the interval $(-M/2f_c, M/2f_c)$ covered by equation (A7). Hence, one obtains the conditions

$$f_c = mf_{NQ} \qquad \text{and} \qquad M \ge mN, \quad \text{(A8)}$$

where m is a positive integer. For the calculations performed in this study, m, M, and N are all integral powers of 2.

[32] For a given value of m (the cutoff frequency), the solution for $E\{\hat{S}_N(f)\}$ may be computed using FFTs of increasing size $2M$ to compute $s(\tau)$. For the problem at hand (see Figure 3), adequate convergence is attained for $M = 2mN$. Setting $M = 2mN$, one may then compute a sequence of solutions of increasing accuracy for $m = 2, 4, 8, \ldots$ The error decreases at each iteration until the desired accuracy is achieved. A relative error on the order of $\varepsilon = 10^{-4}$ is obtained for $m = 4096$ in the case $1.7 \le \alpha \le 2$. (For the large values of N considered here calculations for $\alpha < 1.7$ could not be performed due to the large sizes of the FFTs involved.) The maximum relative error occurs near the endpoints of the interval, that is, near the Nyquist frequency. For calculations in which $m = 4096$, $M = 2mN$, and $N = 2^{16}$, the maximum relative error is estimated from the numerical data to be roughly 2×10^{-4}, 4×10^{-4}, and 9×10^{-4} for $\alpha = 1.9$, 1.8, and 1.7, respectively.

[33] **Acknowledgments.** I would like to thank D. A. Roberts for thoughtful comments and the two referees for several recommendations that led to an improved presentation of the results.

[34] Shadia Rifai Habbal thanks Don B. Percival and Roberto Bruno for their assistance in evaluating this paper.

References

Bavassano, B., M. Dobrowolny, F. Mariani, and N. F. Ness (1982), Radial evolution of power spectra of interplanetary Alfvénic turbulence, *J. Geophys. Res.*, *87*, 3617.

Goldstein, M. L., and D. A. Roberts (1999), Magnetohydrodynamic turbulence in the solar wind, *Phys. Plasmas*, *6*, 4154.

Goldstein, M. L., D. A. Roberts, and W. H. Matthaeus (1995), Magnetohydrodynamic turbulence in the solar wind, *Annu. Rev. Astron. Astrophys.*, *33*, 283.

Leamon, R. J., C. W. Smith, N. F. Ness, W. M. Matthaeus, and H. K. Wong (1998), Observational constraints on the dynamics of the interplanetary magnetic field dissipation range, *J. Geophys. Res.*, *103*, 4775.

Levinson, N., and R. M. Redheffer (1970), *Complex Variables*, McGraw-Hill, New York.

Marsch, E. (1991), MHD turbulence in the solar wind, in *Physics of the Inner Heliosphere*, vol. 2, edited by R. Schwenn and E. Marsch, p. 159, Springer, New York.

Matthaeus, W. H., and M. L. Goldstein (1982), Measurement of the rugged invariants of magnetohydrodynamic turbulence in the solar wind, *J. Geophys. Res.*, *87*, 6011.

McComas, D. J., S. J. Bame, P. Barker, W. C. Feldman, J. L. Phillips, P. Riley, and J. W. Griffee (1998), Solar Wind Electron Proton Alpha Monitor (SWEPAM) for the Advanced Composition Explorer, *Space Sci. Rev.*, *86*, 563.

Percival, D. B., and A. T. Walden (1993), *Spectral Analysis for Physical Applications*, Cambridge Univ. Press, New York.

Priestley, M. B. (1981), *Spectral Analysis and Time Series*, vols. 1 and 2, Elsevier, New York.

Thomson, D. J. (1977), Spectrum estimation techniques for characterization and development of WT4 waveguide–II, *Bell Sys. Tech. J.*, *56*, 1983.

Thomson, D. J. (1982), Spectrum estimation and harmonic analysis, *Proc. IEEE*, *70*, 1055.

Tu, C.-Y., and E. Marsch (1995), MHD structures, waves and turbulence in the solar wind: Observations and theories, *Space Sci. Rev.*, *73*, 1.

J. J. Podesta, NASA Goddard Space Flight Center, Laboratory for Solar and Space Physics, Code 612.2, Greenbelt, MD 20771, USA. (jpodesta@solar.stanford.edu)